



Sonolytic and sonophotolytic degradation of Carbamazepine: Kinetic and mechanisms



Yongfang Rao^{a,*}, Haisong Yang^a, Dan Xue^a, Yang Guo^b, Fei Qi^b, Jun Ma^{c,*}

^a Department of Environmental Science and Engineering, Xi'an Jiaotong University, Xi'an 710049, PR China

^b College of Environmental Science and Engineering, Beijing Forestry University, Beijing 100083, PR China

^c State Key Laboratory of Urban Water Resource and Environment, Harbin Institute of Technology, Harbin 150090, PR China

ARTICLE INFO

Article history:

Received 21 September 2015

Received in revised form 3 April 2016

Accepted 4 April 2016

Available online 4 April 2016

Keywords:

Carbamazepine

Ultrasound

Sonophotolysis

Hydroxyl radicals

Decay pathways

ABSTRACT

An in-depth investigation on the ultrasonic decomposition of Carbamazepine (CBZ), one of the most regularly identified drugs in the environment, was conducted. The effects of diverse variables were evaluated, such as frequency, power, solution pH, initial CBZ concentration and varied inorganic anions. Reaction order was determined on the basis of analyzing reaction kinetics of CBZ degradation. The sonophotolysis and photolysis of CBZ was also examined in this contribution. The influence of water composition on the sonolytic and sonophotolytic elimination of CBZ was analyzed. Additionally, 21 intermediates were identified during sonolytic degradation of CBZ based on LC/ESI-MS/MS analysis, among which two escaped from the detection in previous studies. Possible decay pathways were proposed accordingly. The epoxidation, cleavage of double bond, hydration, hydroxylation, ring contraction and intramolecular cyclization were believed to be involved in sonochemical degradation of CBZ.

© 2016 Elsevier B.V. All rights reserved.

1. Introduction

Pharmaceuticals have attracted intensive concerns as emerging pollutants in aquatic environment in recent years. Owing to ever-increasing consumption, inappropriate disposal and their incomplete removal in wastewater treatment plants (WWTPs), pharmaceuticals have been found ubiquitously in natural waters [1,2]. Although most pharmaceuticals exist in the aquatic environment at trace level and show relatively low acute toxicity, it is possible that there are synergistic effects of pharmaceutical mixtures [3] and continuous exposure to these compounds leads to negative impact on ecosystem.

Carbamazepine (CBZ) is a prescription drug which is used to treat seizure disorders, alleviation of neuralgia, and various psychiatric disorders. The annual usage of CBZ ranks the second among all the antiepileptic drugs in China [4]. CBZ is frequently found in different waters including surface water (up to 3.09 µg/L) [5,6], ground water (up to 610 ng/L) [7] and drinking water (up to 30 ng/L) [8] because it can survive in WWTPs and persist for a long time in aquatic environment. Previous studies reported that the eradication of CBZ in WWTPs was generally inefficient [9]. Therefore, CBZ has been used as an anthropogenic marker for

water contamination in the environment [10,11]. It was reported that environmentally-relevant concentrations of CBZ could negatively influence aquatic life such as bacteria, algae, invertebrates, and fish [12–15] as well as change freshwater community structure, ecosystem dynamics and coastal systems [16,17].

These facts have drawn extensive interests into the investigation of CBZ degradation by various advanced oxidation processes (AOPs) such as Ozonation [18], $\text{Fe}^{2+}/\text{S}_2\text{O}_8^{2-}$ [19], UV/ H_2O_2 [20], photo-Fenton procedure [21], Electrochemical oxidation [22] and photocatalysis [23,24]. Compared to these more established AOPs, ultrasonic irradiation offers an alternative method that is simpler and more environment-friendly because Ultrasound treatment process is chemical-free, easy to operate and causes no secondary pollution [25,26]. Both physical and chemical processes can be triggered by the propagation of Ultrasound through acoustic cavitation, including the configuration, expansion and adiabatically implosive breakdown of microbubbles in the liquid. The rapid breakdown of cavitation bubbles is coupled with adiabatic heating of the vapor phase of the bubble that yields high local transitory temperatures (estimated to be around 4200 K) and pressures (estimated to be around 975 bar) [27]. Water molecules under these extreme conditions suffers a thermal breakdown to generate the exceedingly reactive radicals $\cdot\text{H}$ and $\cdot\text{OH}$, and yields HO_2 in the existence of O_2 [28]. Thus, organic compounds in close proximity to the bubble/water interface can be subjected to thermal

* Corresponding authors.

E-mail addresses: yfiao@mail.xjtu.edu.cn (Y. Rao), majun@hit.edu.cn (J. Ma).

decomposition, and/or secondary reactions between the reactive radicals and them, leading to their degradation and even mineralization. Ultrasonic treatment of CBZ has been reported at the fixed frequency of 520 kHz in a previous study [29].

This contribution has made a more comprehensive investigation on CBZ degradation by Ultrasound and UV/Ultrasound processes. The influence of diverse variables has been evaluated including Ultrasound frequencies, power, pH, CBZ initial concentration and inorganic anions. CBZ degradation has also been examined by UV, Ultrasound and UV/Ultrasound processes in pure water and secondary effluent wastewater. This study also identified the intermediates or products generated during CBZ destruction and possible degradation pathways were proposed accordingly.

2. Materials and methods

2.1. Chemicals

CBZ and Carbamazepine 10,11-epoxide were obtained from Tokyo Chemical Industry and Fluka, respectively. All other chemicals are of analytic purity and all solvents are of HPLC grade purity. Sulfuric acid and Sodium hydroxide were used for pH adjustment. Distilled-Deionized water (DDW) was used exclusively in this study.

2.2. Ultrasonic, UV and sonophotolytic systems

Sonolytic experiments were conducted in a cylindrical glass beaker with an effective volume of 500 mL, which was placed on transducers working at two resonant frequencies (200, 400 kHz). Each transducer is connected to a high-frequency power supply, which was made by Shanghai Acoustics Lab, Chinese Academy of Sciences, China. The nominal input power can be regulated manually by the control panel. The temperature during ultrasonic process was controlled at $20\text{ }^{\circ}\text{C} \pm 3$ by a circulated water bath. Fig. 1 is a schematic of the experiment apparatus. Aliquots (1 mL) of reaction solution were taken from the reactor at prearranged time intervals for further analysis. All experiments were carried out in duplicate and the error is less than 5.0%.

A home-made aluminum photoreaction chamber was used for the photolytic reactor, in which two lamps are fixed on the ceiling of the chamber. In addition, a cooling blower was furnished in the chamber to control temperature. The monochromatic ultraviolet light wavelength of low-pressure mercury lamps employed in this study was 253.7 nm since the absorption of H_2O_2 at $\lambda > 300$ nm nearly approaches zero [30]. In order to guarantee a stable UV

output, the lamps were warmed up for 5 min before the initiation of each experiment. The surface irradiance was determined to be 2.74×10^{-7} Einsteins $\text{L}^{-1} \text{s}^{-1}$ by iodide–iodate actinometry [31]. The optical path length is determined to be 10.16 ± 0.04 cm by quantifying the photolytic rate of H_2O_2 [32].

The sonophotolytic experiments were conducted by placing the sonolytic setup inside the photo-chamber as shown in Fig. 1, so that both the Ultrasound and UV could be employed concurrently.

2.3. Analytic methods

The remaining CBZ after reaction was determined by HPLC, which was comprised of a Yilite P230 HPLC pump, a Yilite UV 230+ UV/vis detector and a RESTEK C18 column (pinnacle DB, 250×4.6 mm, and $5\text{ }\mu\text{m}$ particle size). The maximum adsorption wavelength (λ_{max}) was selected as 210 nm for CBZ. An isocratic flow of acetonitrile/DDW (60/40) was used as the mobile phase running at a flow rate of 1.0 mL/min. The concentration of H_2O_2 was determined colorimetrically using a UV–vis spectrophotometer at 405 nm after adding Titanium oxysulfate to form titanium peroxide (TiO_2^{2+}) [33].

The identification of intermediates was carried out with an initial CBZ concentration at 0.15 mM. The intermediates were identified by a UPLC/ESI-MS/MS system equipped with Bruker amaZon SL ion trap mass analyzer and Dionex UltiMate 3000 Ultra-high Performance Liquid Chromatography (UPLC). The Thermo Hypersil GOLD column ($1.9\text{ }\mu\text{m}$, 50×2.1 mm) was used for UPLC. A gradient method set at a flow rate of 0.2 mL min^{-1} was used with the eluent consisting of A (0.1% formic acid) and B (100% acetonitrile). Component A was maintained at 95% during the first 2 min, then B was steadily increased from 5% to 85% in the next 10 min and B was maintained at 85% in the next 2 min.

2.4. Toxicity assays

The unicellular green microalgae *Chlorella vulgaris* (*C. vulgaris*) was obtained from the Chinese Research Academy of Environmental Sciences and used to evaluate the algae toxicity according to the method previously described by Essam et al. [34] and our previous study [35]. Different solution samples were added individually to the algae growth medium (M-11). Following their inoculation with *C. vulgaris* in exponential phase, the test tubes were sealed with gauzes and cultured in artificial climate incubators (2000 lux, light:dark = 12 h:12 h and 298 ± 1 K). Growth was monitored periodically up to 96 h by measuring the algae cell concentration directly using an optical microscope (Chongqing Optec Instrument Co. Ltd, China). The inhibition test of *C. vulgaris* is calculated as follows:

$$I_y = \frac{Y_B - Y_A}{Y_B}$$

where Y_A and Y_B represent the average algae cell concentrations of three parallel *C. vulgaris* solutions and a blank solution, respectively, under the same culture conditions. The 96-EC₅₀ values, which represent the effective concentrations required to provide 50% inhibition, were determined in 96-well plates.

3. Results and discussion

3.1. Effects of ultrasonic frequency and CBZ degradation mechanism by ultrasound

Ultrasonic frequency is a crucial parameter which can influence the performance of sonolysis since it considerably affects the size and the duration of cavitation bubbles, consequently influencing

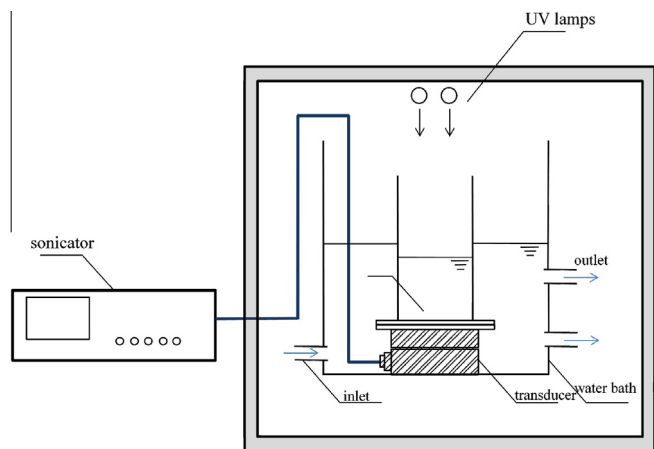


Fig. 1. The diagram of the experimental setup.

the number of cavitation bubbles, the violence of bubble breakdown, and the production of hydroxyl radical [36]. The number of cavitation bubbles and bubble collapses increase with the growth of the frequency. However, the bubbles generated at high-frequency are small and release less energy than the low-frequency bubbles do for one single pulse [37]. Therefore, the optimal frequency is determined by the comprehensive performance of energy discharge which depends on the amount, bubble size and lifetime of bubbles, and the optimal frequency may differ for different compounds [38,39]. CBZ degradation was investigated at two different ultrasonic frequencies. As shown in Fig. 2a, CBZ ultrasonic degradation was found to follow pseudo first-order kinetics ($R^2 > 0.99$). The faster degradation rate of CBZ was observed for ultrasound at 200 kHz (k_{obs} , $0.028 \pm 0.001 \text{ min}^{-1}$) than that at 400 kHz (k_{obs} , $0.0158 \pm 0.0008 \text{ min}^{-1}$).

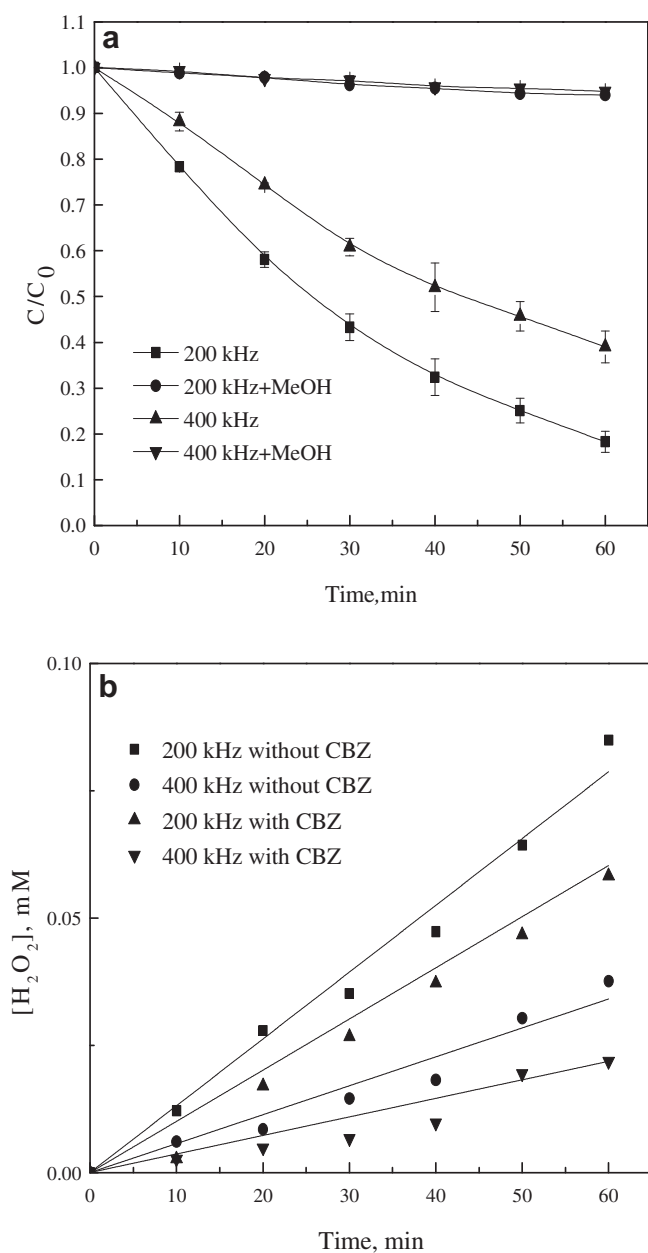


Fig. 2. (a) Effects of US frequency and radical scavengers. (b) Effects of US frequency on the generation of H_2O_2 . ($[\text{CBZ}]_0 = 0.025 \text{ mM}$; US: 100 W; reaction volume is 200 mL; no pH adjustment).

It is widely acknowledged that two mechanisms may involve in the sonolytic degradation of organic compounds: pyrolysis and hydroxyl radicals oxidation. The degradation mechanisms vary with the target compounds [40,41]. In order to elucidate the mechanisms of CBZ sonolysis, CBZ degradation was examined in the presence of 1.0 M methanol, an effective quencher for hydroxyl radicals. As indicated in Fig. 2, the addition of methanol remarkably diminished CBZ degradation by ultrasound both at 200 kHz and 400 kHz, implying hydroxyl radicals play a dominating role in CBZ sono-degradation. CBZ cannot be pyrolyzed inside the cavitation bubbles in view of the fact that its Henry's law constant was approximately $1.08 \times 10^{-10} \text{ atm} \cdot \text{m}^3/\text{mol}$ [42], indicating low fugacity. In addition, due to its low water solubility (112 mg/L) and high Log P (2.45) which is Octanol–water partition coefficient [42], CBZ may exist at the interface of bubble-bulk solution. Therefore, hydroxyl radical is the key player responsible for CBZ degradation by Ultrasound.

Besides the degradation process, the sonolytic treatment also generated H_2O_2 . The quantity of H_2O_2 generated by sonolysis was determined in water with and without CBZ at 200 and 400 kHz. Due to the consumption of hydroxyl radicals by CBZ, the concentration of H_2O_2 generated is lower in CBZ solution than that in DDW at both 200 and 400 kHz as illustrated in Fig. 2b. The formation rate of H_2O_2 ($1.31 \pm 0.06 \mu\text{mol L}^{-1} \text{ min}^{-1}$) at 200 kHz is much faster than that ($0.568 \pm 0.03 \mu\text{mol L}^{-1} \text{ min}^{-1}$) at 400 kHz in CBZ-free DDW. The formation rate of H_2O_2 ($0.932 \pm 0.05 \mu\text{mol L}^{-1} \text{ min}^{-1}$) at 200 kHz is much faster than that ($0.329 \pm 0.02 \mu\text{mol L}^{-1} \text{ min}^{-1}$) at 400 kHz in 0.025 mM CBZ solution. These indicate the formation rate of hydroxyl radicals is faster at 200 kHz than that at 400 kHz in both DDW and CBZ solution. Furthermore, the calorimetric power at both 200 and 400 kHz for the 100 W setting was measured and calculated by Eq. (1). The calorimetric power at 400 kHz is 11.4 W for the 100 W setting, which is much lower than that (46.4 W) at 200 kHz. This may also rationalize slower CBZ degradation rate at 400 kHz. Therefore, the sonicator with the frequency at 200 kHz was used for CBZ sono-degradation in the following part.

3.2. Effect of the ultrasonic power

The applied power is a critical parameter which can determine the performance of sonolysis. In this study, the effect of applied electric power ranging from 20 to 100 W was evaluated on CBZ degradation with CBZ concentration fixed at 0.025 mM and pH value fixed at 6.0. Additional experiments were conducted to assess the actual power dissipating in the reaction solution (acoustic power) by the calorimetric method based on Eq. (1) [43].

$$\text{Acoustic power (W)} = (dT/dt) \cdot C_p \cdot M \quad (1)$$

where C_p is the specific heat of water ($4200 \text{ J/kg}^\circ\text{C}$), and M is the mass of water (kg). The results are summarized in Table 1. The actual power absorbed by the reaction solution accounts for more than 42% of the applied electric power. Fig. 3a describes the effect of applied electric power on CBZ degradation. The degradation rate of CBZ crescendo with the increment of the applied power in a linear relationship as shown in the inset of Fig. 3. It is interesting to

Table 1
Sonochemical efficiencies at different power.

Parameters	Unit	Electric power (W)				
		20	40	60	80	100
Water volume	mL	200	200	200	200	200
Sonolysis time	min	10	10	10	10	10
Acoustic power	W	8.8	17.4	25.6	34.1	46.4
Acoustic efficiency	%	44.0	43.5	42.7	42.6	46.4

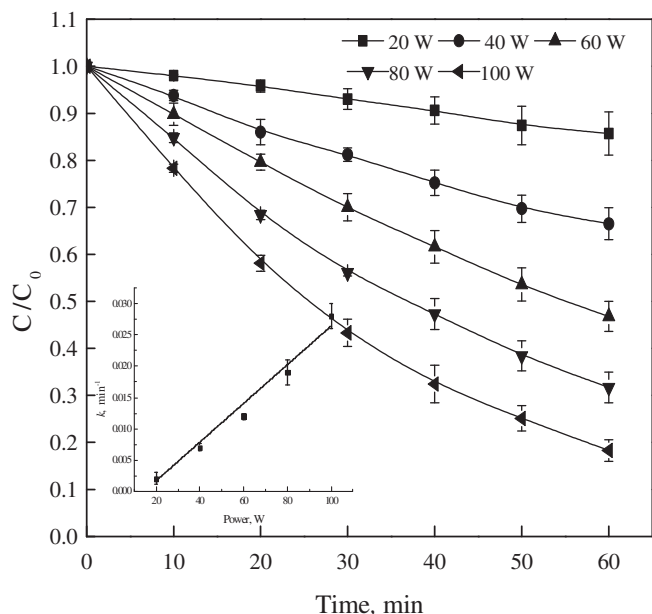


Fig. 3. Effects of US power, where the inset describes k VS power. ($[CBZ]_0 = 0.025$ mM; US: 200 kHz; no pH adjustment).

note that the linear line fails to pass through the original point (see the inset of Fig. 3). This may be because ultrasound with low power could not generate enough radicals to oxidize CBZ. According to the inset of Fig. 3a, the power threshold can be determined to be 16 W. The establishment of the linear correlation between k_{obs} and power renders the prediction of CBZ sono-degradation possible.

3.3. Effect of initial pH levels

The pH value is generally a vital parameter in water and wastewater treatment. How initial pH levels affect CBZ reduction was evaluated ranging from 2.0 to 11.0, and the results are presented in Fig. 4. Varying pH from 4.5 to 11.0 has no significant

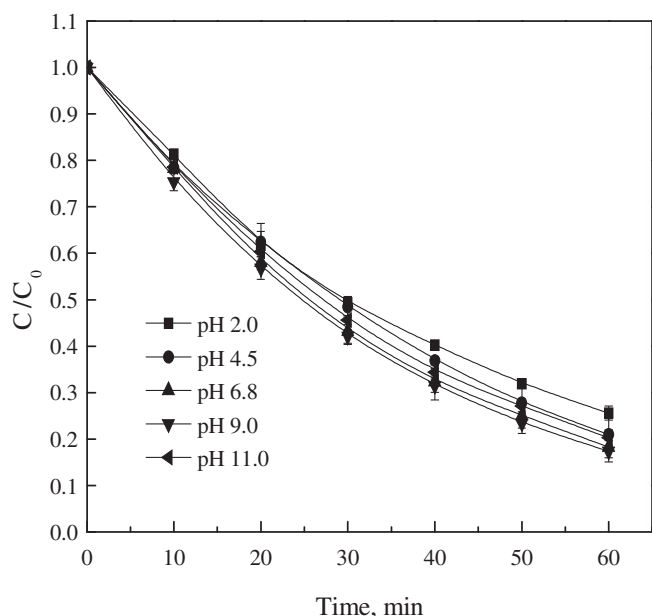


Fig. 4. Effects of pH levels ($[CBZ]_0 = 0.025$ mM; US: 200 kHz–100 W; reaction volume is 200 mL).

effect on CBZ degradation by Ultrasound. CBZ degradation was slightly reduced at pH 2.0. Since CBZ is a non-volatile organics, the place where it was degraded is the interface of cavitation bubbles and bulk solution. Consequently, CBZ decay rate would be accelerated if its hydrophobicity is promoted. CBZ shows a hydrophobic property when it retains a molecular structure. Moreover, it has a pK_{a1} of 2.3 related to the protonation of the NH_2 group and pK_{a2} of 13.9 related to the deprotonation of the amino group [44]. More than half of CBZ exist in ionized state at pH 2.0, and this leads to the enhancement of its hydrophilicity and solubility which in turn hampers CBZ in reaching the exterior of the cavitation bubbles. Thus, part of CBZ degradation reaction happens in the bulk solution where lower concentration of hydroxyl radicals appears. And the emergence of the lower concentration of hydroxyl radicals is attributed to the approximately 10% of hydroxyl radicals generated in the cavitation bubbles diffusing into the bulk solution [45]. On the other hand, the structure of CBZ is in the molecular state when pH ranging from 4.5 to 11.0 is not near the two pK_a values of CBZ, which favors CBZ molecules arriving at the exterior of the bubbles.

3.4. Effect of initial CBZ concentration and the determination of reaction order

CBZ degradation was investigated at different initial concentration by sole-US process ranging from 0.00625 to 0.1 mM (see Fig. 5a). CBZ removal efficiency is inversely proportional to the initial concentration. However, it is interesting to observe the total removal of CBZ increased is directly proportional to the initial concentration as demonstrated in the inset of Fig. 5a.

As described earlier, the principal mechanism of CBZ degradation by Ultrasound is the oxidation of hydroxyl radicals at the bubble/bulk interface and in the bulk solution. CBZ degradation reaction can be described as follows:



Thus, CBZ degradation rate can be written as follows:

$$-\frac{d[\text{CBZ}]}{dt} = xk_{\text{CBZ, OH}}[\text{CBZ}]^x[\text{HO}^\bullet] \quad (3)$$

With a constant power input, the generation rate of HO^\bullet is supposed to be constant during sonolysis. And the HO^\bullet concentration in the solution can be assumed to maintain a steady state during the reaction since hydroxyl radicals do not accumulate to an appreciable level in the solution. Thus, CBZ decay rate can be redefined as Eq. (4):

$$-\frac{d[\text{CBZ}]}{dt} = xk[\text{CBZ}]^x \quad (4)$$

where $k = k_{\text{CBZ, OH}}[\text{HO}^\bullet]$. At the initial stage, initial decomposition rate of CBZ can be described as:

$$-\frac{d[\text{CBZ}]_0}{dt} = xk[\text{CBZ}]_0^x \quad (5)$$

Taking logarithms of both sides of Eq. (5) yields:

$$\ln\left(-\frac{d[\text{CBZ}]_0}{dt}\right) = \ln kx + x\ln[\text{CBZ}]_0 \quad (6)$$

The x can be determined to be 0.659 ± 0.0318 by plotting $\ln\left(-\frac{d[\text{CBZ}]_0}{dt}\right)$ at different $[\text{CBZ}]_0$ as a function of the CBZ initial concentration as shown in Fig. 5b. Thus, CBZ degradation reaction can actually be described as Eq. (7):



Based on Eq. (7), CBZ degradation is supposed to follow first-order kinetics since HO^\bullet concentration remains constant in the solution,

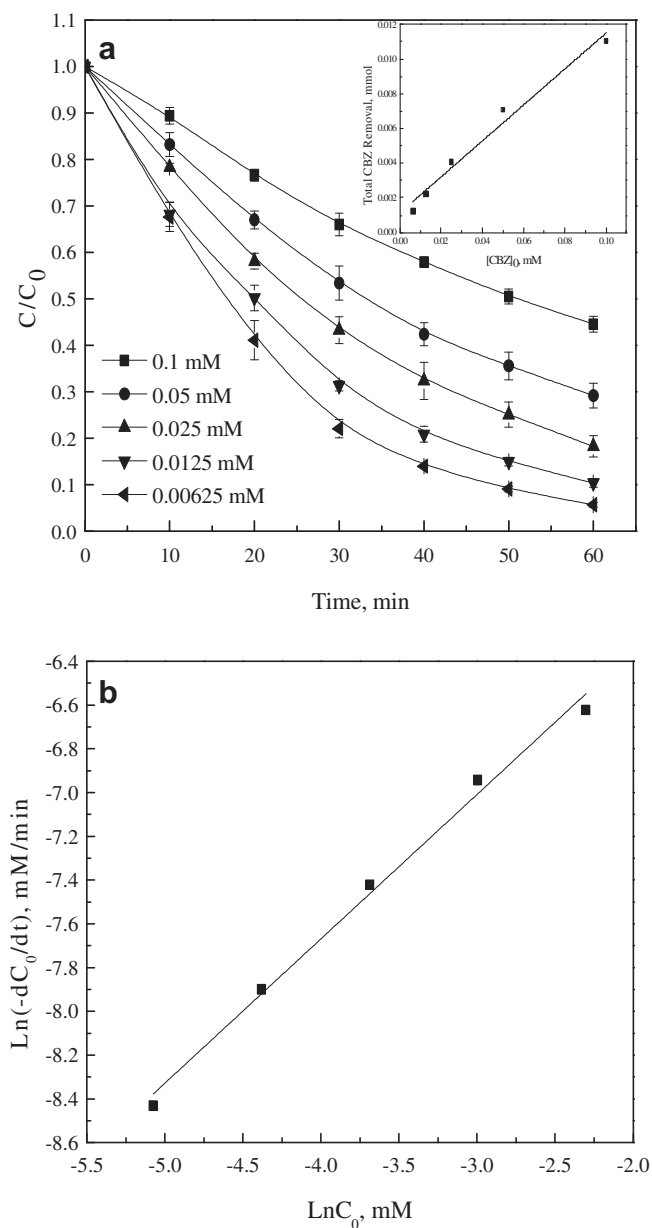


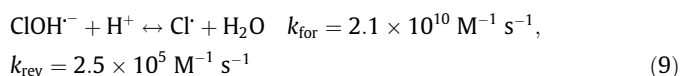
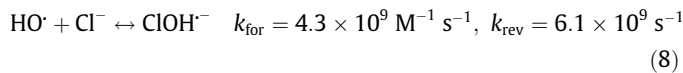
Fig. 5. (a) Effects of initial CBZ concentration, where the inset describes total removal VS initial concentration. (b) $\ln(-dC_0/dt)$ vs $\ln C_0$. (US: 200 kHz–100 W; reaction volume is 200 mL; no pH adjustment).

and this was confirmed in our study. Furthermore, the intercept reveals $\ln k$ to be around -5.03 ± 0.121 . Then k can be calculated to be 0.01023 ± 0.0005 . As described earlier, the k equals $k_{CBZ, HO}[HO^\cdot]$ in number. The $k_{CBZ, HO}$ has been reported to be $2.98 \times 10^9 \text{ M}^{-1} \text{ s}^{-1}$ [24]. Thus, $[HO^\cdot]$ at a steady state can be approximately determined to be $(3.43 \pm 0.16) \times 10^{-12} \text{ M}$.

3.5. Effect of inorganic anions

The influence of various inorganic anions was also evaluated on the performance of CBZ sono-degradation. It has reported that anions such as chloride ions exert different effects on the removal of different compounds by advanced oxidation processes (AOPs) in previous studies [46–48]. In our previous studies [19], the presence of Cl^- significantly promoted CBZ degradation by $Fe^{2+}/S_2O_8^{2-}$ process and the promoting effects increased with the enhancement of Cl^- concentration due to the generation of the additional

radicals such as Cl^\cdot and Cl_2^\cdot . In this process, hydroxyl radicals are believed to make major contribution to CBZ sono-degradation. They can also oxidize Cl^- to generate Cl^\cdot and Cl_2^\cdot through a series of chain reactions as described in Eqs. (8)–(10) [49]:



However, different experimental results were observed as illustrated in Fig. 6. The Cl^- slightly restrained CBZ degradation while SO_4^{2-} and NO_3^- exerted no influence on CBZ decomposition by Ultrasound. This can be rationalized by the facts that most hydroxyl radicals exist at the exterior of cavitation bubbles which is not accessible for Cl^- . The slight inhibiting effect of Cl^- may be because chloride ions may consume the trace HO^\cdot in the bulk solution to produce $ClOH^\cdot$ as described in Eq. (8). On the other hand, $[H^+]$ is low at pH 6.8, which is not favorable for the forward direction of Eq. (9), repressing the generation of Cl^\cdot and Cl_2^\cdot . Sulfate ions and nitrate ions were reported to negatively influence the performance of advanced oxidation processes since the high ion strength may hinder the electron transfer during the oxidation reaction. In this process, CBZ degradation reaction took place at the exterior of cavitation bubbles which is not accessible for SO_4^{2-} and NO_3^- . Therefore, no measurable influence of these two ions was observed on CBZ sono-degradation.

3.6. CBZ degradation by sole-UV and UV/Ultrasound processes

In this study, we also examine CBZ decomposition under UV irradiation and simultaneous irradiation by UV and Ultrasound as indicated in Fig. 7. Initial concentration of CBZ was fixed at 0.025 mM without pH adjustment. The power and frequency of Ultrasound was fixed at 100 W and 200 kHz, respectively. The surface irradiance of UV was $2.74 \times 10^{-7} \text{ Einsteins L}^{-1} \text{ s}^{-1}$.

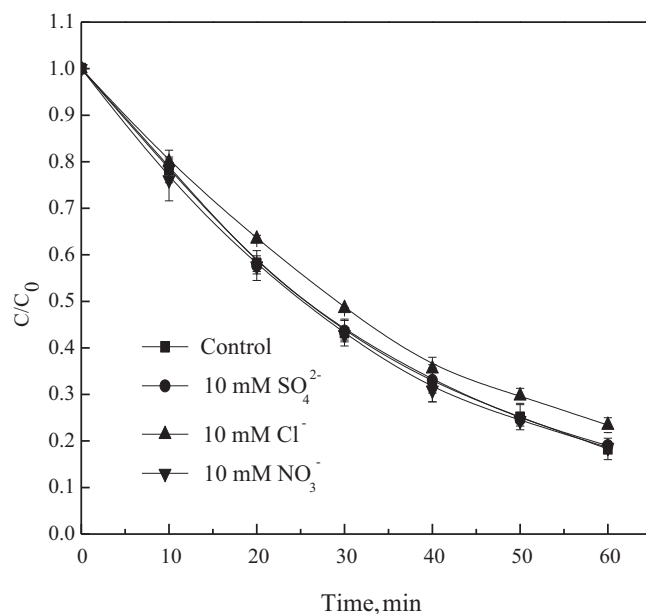


Fig. 6. Effects of inorganic anions ($[CBZ]_0 = 0.025 \text{ mM}$; US: 200 kHz–100 W; reaction volume is 200 mL; no pH adjustment).

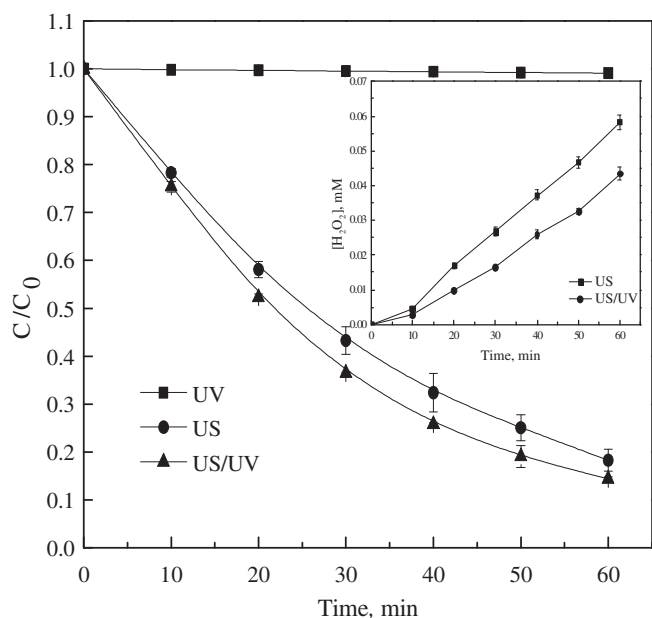


Fig. 7. CBZ degradation by various processes, where the inset is comparison between the generation of H₂O₂ in US and UV/US processes. ([CBZ]₀ = 0.025 mM; US: 200 kHz–100 W; UV: λ = 253.7 nm; UV intensity is 2.74×10^{-7} Einsteins L⁻¹ s⁻¹; reaction volume is 200 mL; no pH adjustment).

CBZ removal was insignificant under sole-UV irradiation (Less than 1% after 60 min). Fig. 7 also shows that the addition of UV irradiation accelerates CBZ degradation (k_{obs} was enhanced from 0.280 ± 0.001 to 0.329 ± 0.002 min⁻¹). It is well known that H₂O₂ can be generated during sonication through a series of chain reactions as described in Eqs. (11)–(16):



Under the irradiation of UV light, the photolysis of H₂O₂ can produce more HO[•]. As demonstrated in the inset of Fig. 7, the concentration of H₂O₂ increased with the sonication time in Ultrasound and UV/Ultrasound systems, and H₂O₂ concentration in UV/ Ultrasound system was lower than that in Ultrasound system due to the photolysis of H₂O₂.

3.7. Effect of water composition on CBZ degradation

Sonolytic and sonophotolytic degradation of CBZ has also been investigated in secondary effluent wastewater (SEW) from a wastewater treatment plant in Xi'an, China. The SEW was passed through a membrane of 0.45 μm pore size to avoid particle effects. COD, pH and NO₃⁻ concentration of SEW is 31.4 mg/L, 7.2 and 37.2 mg/L, respectively. As indicated in Fig. 8, sonolytic degradation of CBZ was depressed in SEW compared to that in DDW while sonophotolytic degradation rate of CBZ in SEW was slightly higher than that in DDW. As described above, hydroxyl radicals dominantly contributed to sonolytic decomposition of CBZ. Organic

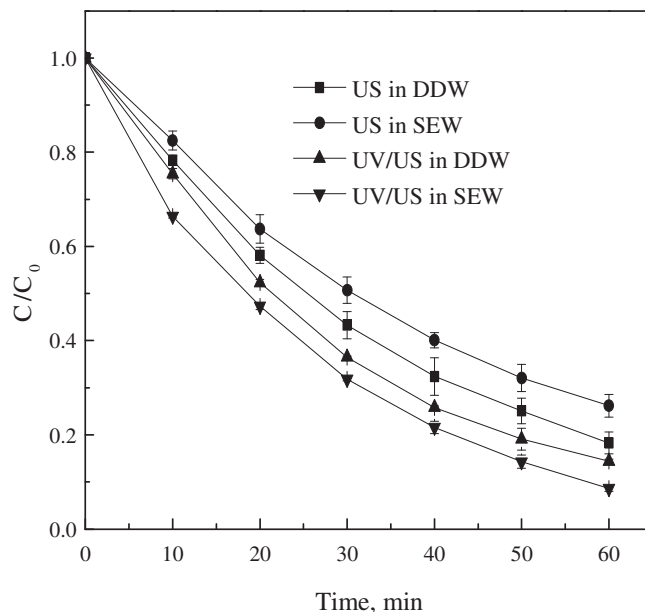


Fig. 8. Effects of water composition on CBZ sonolysis and sonophotolysis ([CBZ]₀ = 0.025 mM; US: 200 kHz–100 W; UV: λ = 253.7 nm; UV intensity is 2.74×10^{-7} Einsteins L⁻¹ s⁻¹; reaction volume is 200 mL; no pH adjustment).

compounds and reducing agents may compete for hydroxyl radicals with CBZ in SEW, leading to less hydroxyl radicals available for CBZ. The promoting effects of SEW may be attributed to the presence of nitrate ions and photo-sensitizers such as humic acid in sonophotolytic degradation of CBZ. The photolysis of NO₃⁻ generates hydroxyl radicals and other radicals under the irradiation of UV light [50]. The presence of nitrate facilitates Ibuprofen degradation in sole-UV system [51]. CBZ removal efficiency was found to be around 10% with the addition of 37 mg/L nitrate under UV irradiation (data not shown), whereas less than 1% of removal efficiency was observed in the absence of nitrate.

3.8. Identification of intermediates and possible sonolytic degradation pathways

During the sonolytic degradation of CBZ, 21 intermediates were detected by LC–MS/MS including two (compounds 20 and 21) which escaped from detection in previous studies (see Fig. 9). Molecular structures were proposed for each intermediate/product on the basis of the molecular ion masses and MS2 fragmentation patterns. There are 12 isomers, among which compounds 5, 6, 7 and 8 share the same m/z of 253, compounds 11, 12 and 13 share the same m/z of 267, the m/z of compounds 15 and 16 is 271 and compounds 19, 20 and 21 share the same m/z of 287. The identity of compound 5 was corroborated according to the comparison between its retention time and that of the authentic compound (Carbamazepine 10, 11-epoxide). Compounds 6, 7 and 8 were believed to be 1-OH-CBZ, 2-OH-CBZ and 3-OH-CBZ, respectively since it is difficult for hydroxyl radicals to attack 4-C of the benzene ring on the CBZ due to the steric effect. An unknown intermediate was also detected with the m/z of 474, which might be a dimer of CBZ.

Possible decay pathways of CBZ are proposed in Fig. 9. Eight primary intermediates (Compounds 4, 5, 6, 7, 8, 9, 15 and 18) were generated upon CBZ degradation, which were triggered by the attack at the olefinic double bond on the central heterocyclic ring and benzene ring by hydroxyl radicals. The assault of hydroxyl radicals on the olefinic double bond of CBZ could produce an epoxide (compound 5). Two hydroxyl radicals simultaneously attacking the

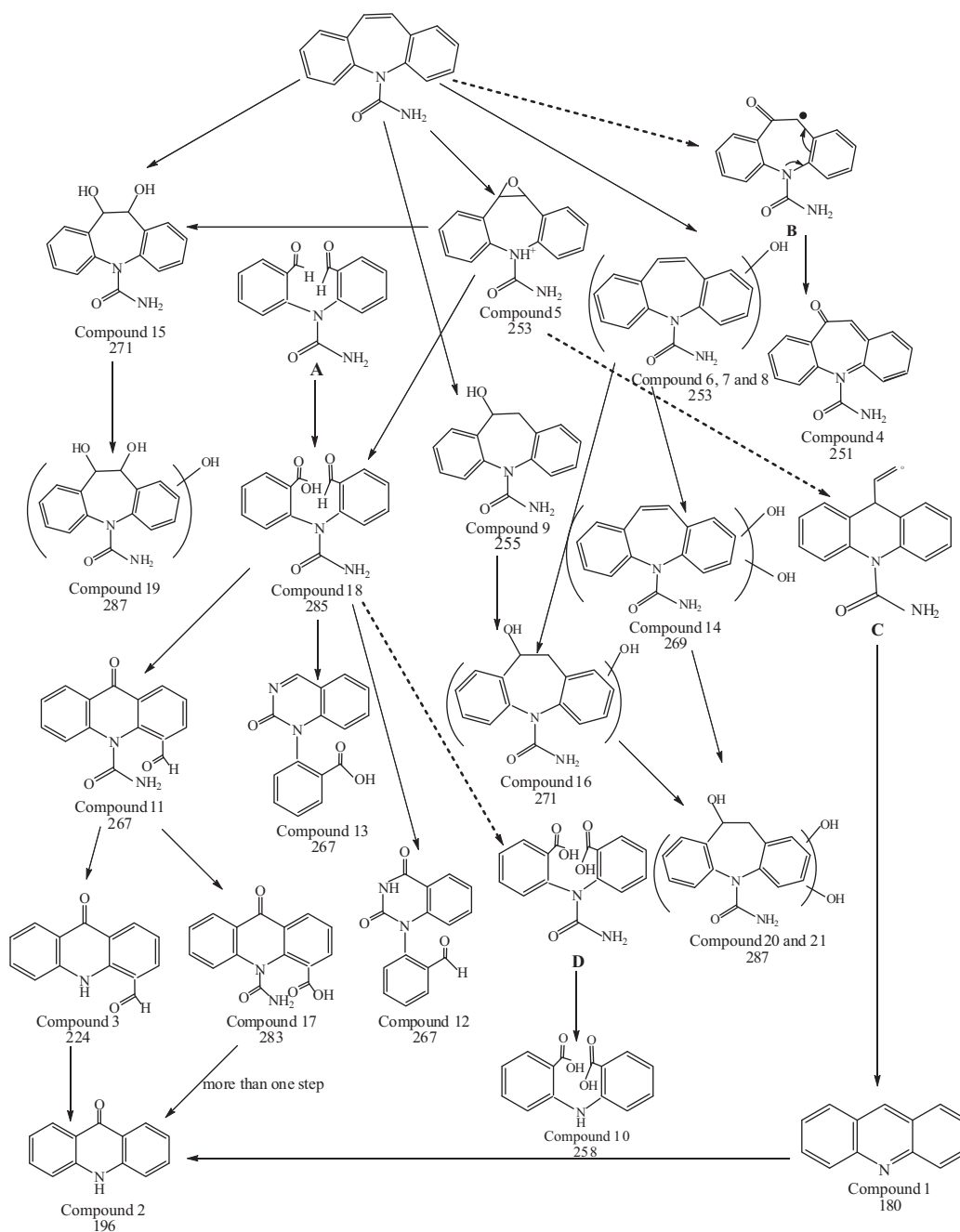


Fig. 9. Possible decay pathways of CBZ by sonication.

olefinic double bond in pairs formed a saturated glycol (compound 15). Hydroxyl radicals may attack olefinic double bond, causing the cleavage of the double bond and the generation of two aldehydes or ketones, such as compound A (not detected though). Compound 18 is believed to come from the further oxidation of compound A. In addition, compounds 15 and 18 might not directly originate from CBZ but from compound 5. To validate this, an additional test was conducted using compound 5 as a starting probe for sonication, where both compounds 15 and 18 were detected. Thus, compounds 15 and 18 could be primary or secondary intermediates. Compound 9 is believed to derive from the hydration of olefinic double bond of CBZ. Oxidation reaction between hydroxyl radicals and the olefinic double bond on the central heterocyclic ring may invite the formation of carbon-centered radical “intermediate B”, which was transformed to compound 5 via rearrange reaction.

The attack of hydroxyl radicals on the benzene ring of CBZ generated compounds 6, 7 and 8. Compound 9 is believed to derive from compound 15 through the attack at the benzene ring of compound 15 by hydroxyl radicals. The formation of “intermediate C (Carbamazepine-9-carboxaldehyde)” can be expected due to the ring contraction of compound 5 as reported in other studies [52]. The subsequent losses of carboxyaldehyde group and CONH₂ lateral chain of “intermediate C” might yield compound 1 (acridine). The further hydroxylation of compound 6, 7 or 8 may generate compound 14. Compound 18 might evolve in four different ways: (1) Intramolecular cyclization via electrophilic aromatic substitution to generate compound 11; (2) the ring closure through intramolecular attack by nitrogen at the aldehyde, leading to the production of compound 13; (3) intramolecular attack by nitrogen at the carbonyl and succeeding dehydration giving compound 12;

Table 2
Toxicity assessment by *Chlorella vulgaris*.

Initial CBZ solution		Solution after 30-min sonication		Solution after 60-min sonication	
Percentage concentration (v/v,%)	Inhibition (%)	Percentage concentration (v/v,%)	Inhibition (%)	Percentage concentration (v/v,%)	Inhibition (%)
0	0	0	0	0	0
20	42.84 ± 0.23	20	51.45 ± 1.05	20	47.36 ± 0.63
40	59.63 ± 1.89	40	67.79 ± 3.37	40	68.26 ± 2.70
60	71.21 ± 2.86	60	87.93 ± 0.31	60	90.20 ± 0.21
96 h-EC ₅₀ = 29.48%		96 h-EC ₅₀ = 18.51%		96 h-EC ₅₀ = 22.47%	

(4) oxidation resulting in the generation of “intermediate D” and the following loss of CONH₂ lateral chain of “intermediate D” to produce compound 10. Compound 3 comes from the loss of CONH₂ lateral chain of compound 11. The further oxidation of compound 11 generates compound 17. Compound 2 (acridone) may arise from three sources: (1) the loss of carboxyaldehyde group on the benzene ring of compound 3; (2) the losses of carboxyl and CONH₂ lateral chain of compound 17; and (3) the oxidation of compound 1. Compound 16 is believed to come from two sources: (1) the assault of hydroxyl radicals at the benzene ring of compound 9; (2) the hydration of compound 6, 7 or 8. Both the further oxidation of compound 16 and hydration of compound 14 may result in the formation of compounds 20 and 21.

3.9. TOC analysis and toxicity assessment

TOC analysis reveals around 10% TOC removal was achieved after 60-min sonication of CBZ with initial concentration of 0.025 mM as shown in Fig. 10, suggesting the mineralization of CBZ by sonication is possible. Toxicological tests were conducted on a solution of CBZ before and after sonication, which were based on the measurement of the inhibition of the growth of *C. vulgaris*, as shown in Table 2. The toxicity assessment for a 96 h-EC₅₀ of CBZ solution before treatment by US is 29.5%. After CBZ was treated by US for 30 min, the 96 h-EC₅₀ decreased to 18.5%, indicating an enhancement in the toxicity of the solution. This is due to the generation of the intermediates such as acridine [53,54], which are more toxic than CBZ. After 60-min sonication, the 96 h-EC₅₀ increase of CBZ solution was observed, suggesting a decrease in

the toxicity compared with the solution after 30-min sonication. This may be due to the decomposition of the intermediates which are more toxic than CBZ. Although the intermediates with higher toxicity were generated during sonolytic degradation of CBZ, sonication is believed to a safe process since the mineralization of CBZ can be achieved.

4. Conclusions

In this contribution, sonolytic and sonophotolytic degradation of CBZ was examined. CBZ degradation followed pseudo first-order kinetics and CBZ degradation rate was faster at a frequency of 200 kHz than that at 400 kHz. The degradation rate is directly proportional to ultrasound power in a linear relationship. Sonolysis of CBZ was slightly depressed at pH 2.0 while pH exerted no significant influence on CBZ degradation at pH levels ranging from 4.5 to 11, indicating that CBZ sonolysis can operate within a wide pH range. CBZ removal efficiency is inversely related to the initial concentration, whereas the total removal of CBZ is directly proportional to the initial concentration. The reaction order of CBZ with hydroxyl radicals was determined to 2.5 during sonolysis. Chloride slightly hampered the sonolysis of CBZ while sulfate and nitrate ions showed no effects on CBZ degradation. The irradiation of UV was observed to stimulate CBZ degradation by Ultrasound. Sonolysis of CBZ was inhibited in secondary effluent wastewater while sonophotolytic degradation of CBZ was accelerated in secondary effluent wastewater. Furthermore, 21 intermediates were identified and sonolytic degradation pathways of CBZ were proposed. All these findings may shed some light on the practical application of sonolysis and sonophotolysis process for CBZ elimination in aqueous phase.

Acknowledgements

The work was supported by Open Project of State Key Laboratory of Urban Water Resource and Environment, Harbin Institute of Technology (No. QA201521) and the Fundamental Research Funds for the Central University, China (No. xjj2012029). The authors are also grateful to all anonymous reviewers who contribute to improving this work.

References

- [1] R.P. Schwarzenbach, B.I. Escher, K. Fenner, T.B. Hofstetter, C.A. Johnson, U. von Gunten, B. Wehrli, The challenge of micropollutants in aquatic systems, *Science* 313 (2006) 1072–1077.
- [2] C.G. Daughton, T.A. Ternes, Pharmaceuticals and personal care products in the environment: agents of subtle change?, *Environ Health Perspect.* 107 (1999) 907–938.
- [3] M. Cleuvers, Mixture toxicity of the anti-inflammatory drugs diclofenac, ibuprofen, naproxen, and acetylsalicylic acid, *Ecotoxicol. Environ. Saf.* 59 (2004) 309–315.
- [4] CMEIN, Chinese medical statistical yearbook. Products section, in, Beijing, China, 2005.
- [5] T.A. Ternes, Occurrence of drugs in German sewage treatment plants and rivers, *Water Res.* 32 (1998) 3245–3260.

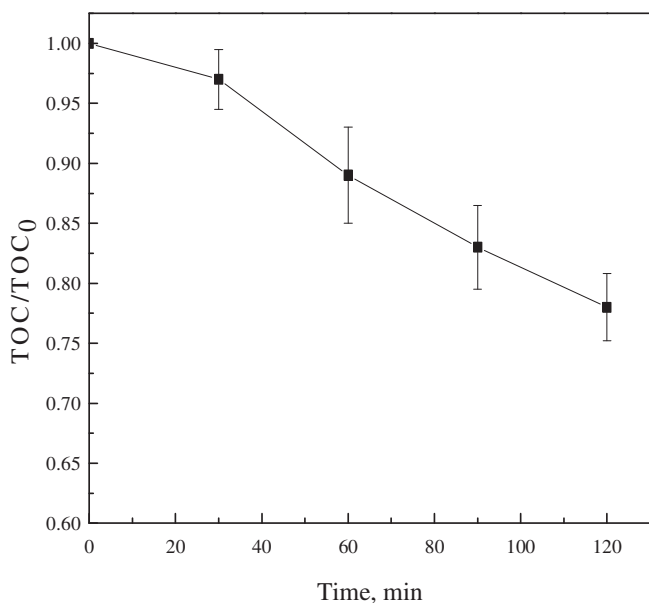


Fig. 10. TOC removal during CBZ degradation by sonication. ([CBZ]₀ = 0.025 mM; US: 200 kHz–100 W; no pH adjustment).

- [6] T. Heberer, Occurrence, fate, and removal of pharmaceutical residues in the aquatic environment: a review of recent research data, *Toxicol. Lett.* 131 (2002) 5–17.
- [7] A. Ginebreda, I. Munoz, M. Lopez de Alda, R. Brix, J. Lopez-Doval, D. Barcelo, Environmental risk assessment of pharmaceuticals in rivers: relationships between hazard indexes and aquatic macroinvertebrate diversity indexes in the Llobregat River (NE Spain), *Environ. Int.* 36 (2010) 153–162.
- [8] T. Heberer, Tracking persistent pharmaceutical residues from municipal sewage to drinking water, *J. Hydrol.* 266 (2002) 175–189.
- [9] Y.J. Zhang, S.U. Geissen, C. Gal, Carbamazepine and diclofenac: removal in wastewater treatment plants and occurrence in water bodies, *Chemosphere* 73 (2008) 1151–1161.
- [10] G. Gasser, M. Rona, A. Voloshenko, R. Shelkov, N. Tal, I. Pankratov, S. Elhanany, O. Lev, Quantitative evaluation of tracers for quantification of wastewater contamination of potable water sources, *Environ. Sci. Technol.* 44 (2010) 3919–3925.
- [11] M. Scheurer, F.R. Storck, C. Graf, H.-J. Brauch, W. Ruck, O. Lev, F.T. Lange, Correlation of six anthropogenic markers in wastewater, surface water, bank filtrate, and soil aquifer treatment, *J. Environ. Monit.* 13 (2011) 966–973.
- [12] B. Ferrari, N. Paxeus, R. Lo Giudice, A. Pollio, J. Garric, Ecotoxicological impact of pharmaceuticals found in treated wastewaters: study of carbamazepine, clofibrac acid, and diclofenac, *Ecotoxicol. Environ. Saf.* 55 (2003) 359–370.
- [13] Z.H. Li, V. Zlabek, J. Velisek, R. Grabic, J. Machova, J. Kolarova, P. Li, T. Randak, Acute toxicity of carbamazepine to juvenile rainbow trout (*Oncorhynchus mykiss*): effects on antioxidant responses, hematological parameters and hepatic EROD, *Ecotoicol. Environ. Saf.* 74 (2011) 319–327.
- [14] H. Chen, J. Zha, X. Liang, J. Li, Z. Wang, Effects of the human antiepileptic drug carbamazepine on the behavior, biomarkers, and heat shock proteins in the Asian clam *Corbicula fluminea*, *Aquat. Toxicol.* 155 (2014) 1–8.
- [15] M. Hampel, J.E. Bron, J.B. Taggart, M.J. Leaver, The antidepressant drug Carbamazepine induces differential transcriptome expression in the brain of Atlantic salmon, *Salmo salar*, *Aquat. Toxicol.* 151 (2014) 114–123.
- [16] A.L. Jarvis, M.J. Bernot, R.J. Bernot, The effects of the psychiatric drug carbamazepine on freshwater invertebrate communities and ecosystem dynamics, *Sci. Total Environ.* 496 (2014) 461–470.
- [17] A. Almeida, V. Calisto, V.I. Esteves, R.J. Schneider, A.M.V.M. Soares, E. Figueira, R. Freitas, Presence of the pharmaceutical drug carbamazepine in coastal systems: effects on bivalves, *Aquat. Toxicol.* 156 (2014) 74–87.
- [18] P. Palo, J.R. Dominguez, J. Sanchez-Martin, Ozonation of a Carbamazepine effluent. Designing the operational parameters under economic considerations, *Water Air Soil Pollut.* 223 (2012) 5999–6007.
- [19] Y.F. Rao, L. Qu, H. Yang, W. Chu, Degradation of carbamazepine by Fe(II)-activated persulfate process, *J. Hazard. Mater.* 268 (2014) 23–32.
- [20] O.S. Keen, S. Baik, K.G. Linden, D.S. Aga, N.G. Love, Enhanced biodegradation of carbamazepine after UV/H₂O₂ advanced oxidation, *Environ. Sci. Technol.* 46 (2012) 6222–6227.
- [21] H.-J. Lee, H. Lee, C. Lee, Degradation of diclofenac and carbamazepine by the copper(II)-catalyzed dark and photo-assisted Fenton-like systems, *Chem. Eng. J.* 245 (2014) 258–264.
- [22] P. Palo, J.R. Dominguez, J. Sanchez-Martin, T. Gonzalez, Electrochemical degradation of carbamazepine in aqueous solutions – optimization of kinetic aspects by design of experiments, *Clean-Soil Air Water* 42 (2014) 1534–1540.
- [23] M.N. Chong, B. Jin, Photocatalytic treatment of high concentration carbamazepine in synthetic hospital wastewater, *J. Hazard. Mater.* 199 (2012) 135–142.
- [24] Y.F. Rao, W. Chu, Y.R. Wang, Photocatalytic oxidation of carbamazepine in triclinic-WO₃ suspension: role of alcohol and sulfate radicals in the degradation pathway, *Appl. Catal. A-Gen.* 468 (2013) 240–249.
- [25] E. Psillakis, G. Goula, N. Kalogerakis, D. Mantzavinos, Degradation of polycyclic aromatic hydrocarbons in aqueous solutions by ultrasonic irradiation, *J. Hazard. Mater.* 108 (2004) 95–102.
- [26] S. Dailianis, V. Tsarpali, K. Melas, H.K. Karapanagioti, L.D. Manariotis, Aqueous phenanthrene toxicity after high-frequency ultrasound degradation, *Aquat. Toxicol.* 147 (2014) 32–40.
- [27] T. Mason, J.P. Lorimer, Sonochemistry: Theory, Applications, and Uses of Ultrasound in Chemistry, Ellis Horwood Ltd., Chichester, U.K., 1988.
- [28] X. Weiping, Q. Yan, L. Dingmin, S. Dan, H. Dewen, Degradation of m-xylene solution using ultrasonic irradiation, *Ultrason. Sonochem.* 18 (2011) 1077–1081.
- [29] T. Nam, P. Drogui, F. Zaviska, S.K. Brar, Sonochemical degradation of the persistent pharmaceutical carbamazepine, *J. Environ. Manage.* 131 (2013) 25–32.
- [30] G.P. Anipsitakis, D.D. Dionysiou, Transition metal/UV-based advanced oxidation technologies for water decontamination, *Appl. Catal. B-Environ.* 54 (2004) 155–163.
- [31] R.O. Rahn, M.I. Stefan, J.R. Bolton, E. Goren, P.S. Shaw, K.R. Lykke, Quantum yield of the iodide-iodate chemical actinometer: dependence on wavelength and concentration, *Photochem. Photobiol.* 78 (2003) 146–152.
- [32] J.H. Baxendale, J.A. Wilson, The photolysis of hydrogen peroxide at high light intensities, *Trans. Faraday Soc.* 53 (1957) 344–356.
- [33] D.W. O'Sullivan, M. Tyree, The kinetics of complex formation between Ti(IV) and hydrogen peroxide, *Int. J. Chem. Kinet.* 39 (2007) 457–461.
- [34] T. Essam, M.A. Amin, O. El Tayeb, B. Mattiasson, B. Guieysse, Solar-based detoxification of phenol and p-nitrophenol by sequential TiO₂ photocatalysis and photosynthetically aerated biological treatment, *Water Res.* 41 (2007) 1697–1704.
- [35] H. Li, B. Xu, F. Qi, D. Sun, Z. Chen, Degradation of bezafibrate in wastewater by catalytic ozonation with cobalt doped red mud: efficiency, intermediates and toxicity, *Appl. Catal. B-Environ.* 152 (2014) 342–351.
- [36] C. Petrier, A. Jeunet, J.L. Luche, G. Reverdy, Unexpected frequency – effects on the rate of oxidative process induced by ultrasound, *J. Am. Chem. Soc.* 114 (1992) 3148–3150.
- [37] C. Petrier, A. Francony, Ultrasonic waste-water treatment: incidence of ultrasonic frequency on the rate of phenol and carbon tetrachloride degradation, *Ultrason. Sonochem.* 4 (1997) 295–300.
- [38] A. Ziyilan, Y. Koltypin, A. Gedanken, N.H. Ince, More on sonolytic and sonocatalytic decomposition of Diclofenac using zero-valent iron, *Ultrason. Sonochem.* 20 (2013) 580–586.
- [39] R. Kidak, S. Dogan, Degradation of trace concentrations of alachlor by medium frequency ultrasound, *Chem. Eng. Process.* 89 (2015) 19–27.
- [40] C.D. Vecitis, H. Park, J. Cheng, B.T. Mader, M.R. Hoffmann, Kinetics and mechanism of the sonolytic conversion of the aqueous perfluorinated surfactants, perfluorooctanoate (PFOA), and perfluorooctane sulfonate (PFOS) into inorganic products, *J. Phys. Chem. A* 112 (2008) 4261–4270.
- [41] L.J. Xu, W. Chu, N. Graham, A systematic study of the degradation of dimethyl phthalate using a high-frequency ultrasonic process, *Ultrason. Sonochem.* 20 (2013) 892–899.
- [42] SRC Phys Prop Database, in, <<http://esc.syrres.com/fatepointer/webprop.asp?CAS=298464>>, 2015.
- [43] T.J. Mason, J.P. Lorimer, D.M. Bates, Quantifying sonochemistry: casting some light on a 'black art', *Ultrason. Sonochem.* 30 (1992) 40–42.
- [44] O.A.H. Jones, N. Voulvoulis, J.N. Lester, Aquatic environmental assessment of the top 25 English prescription pharmaceuticals, *Water Res.* 36 (2002) 5013–5022.
- [45] M. Goel, H.Q. Hu, A.S. Mujumdar, M.B. Ray, Sonochemical decomposition of volatile and non-volatile organic compounds – a comparative study, *Water Res.* 38 (2004) 4247–4261.
- [46] J.E. Grebel, J.J. Pignatello, W.A. Mitch, Effect of halide ions and carbonates on organic contaminant degradation by hydroxyl radical-based advanced oxidation processes in saline waters, *Environ. Sci. Technol.* 44 (2010) 6822–6828.
- [47] Y.R. Wang, W. Chu, Degradation of a xanthene dye by Fe(II)-mediated activation of Oxone process, *J. Hazard. Mater.* 186 (2011) 1455–1461.
- [48] Y. Yang, J.J. Pignatello, J. Ma, W.A. Mitch, Comparison of halide impacts on the efficiency of contaminant degradation by sulfate and hydroxyl radical-based advanced oxidation processes (AOPs), *Environ. Sci. Technol.* 48 (2014) 2344–2351.
- [49] G.G. Jayson, B.J. Parsons, A.J. Swallow, Some simple, highly reactive, inorganic chlorine derivatives in aqueous solution-their formation using pulses of radiation and their role in mechanism of Fricke Dosimeter, *J. Chem. Soc. Faraday Trans.* (1973) 1597–1607.
- [50] J. Mack, J.R. Bolton, Photochemistry of nitrite and nitrate in aqueous solution: a review, *J. Photochem. Photobiol. A – Chem.* 128 (1999) 1–13.
- [51] Y.F. Rao, D. Xue, H.M. Pan, J.T. Feng, Y.J. Li, Degradation of Ibuprofen by a synergistic UV/Fe(III)/Oxone process, *Chem. Eng. J.* 283 (2016) 65–75.
- [52] D. Vogna, R. Marotta, R. Andreozzi, A. Napolitano, M. d'Ischia, Kinetic and chemical assessment of the UV/H₂O₂ treatment of antiepileptic drug carbamazepine, *Chemosphere* 54 (2004) 497–505.
- [53] T. Kosjek, H.R. Andersen, B. Kompare, A. Ledin, E. Heath, Fate of Carbamazepine during water treatment, *Environ. Sci. Technol.* 43 (2009) 6256–6261.
- [54] S. Chiron, C. Minero, D. Vione, Photodegradation processes of the Antiepileptic drug carbamazepine, relevant to estuarine waters, *Environ. Sci. Technol.* 40 (2006) 5977–5983.